

Do Growers Using Solo Fungicides Affect the Durability of Disease Control of Growers Using Mixtures and Alternations? The Case of Spot-Form Net Blotch in Western Australia

Joe Helps,^{1,†} Francisco Lopez-Ruiz,² Ayalsew Zerihun,² and Frank van den Bosch²

¹ Rothamsted Research, Harpenden, AL5 2JQ, U.K.

² Centre for Crop and Disease Management, School of Molecular and Life Sciences, Curtin University, Perth, WA 6845, Australia

Accepted for publication 13 October 2023.

Abstract

Growers often use alternations or mixtures of fungicides to slow down the development of resistance to fungicides. However, within a landscape, some growers will implement such resistance management methods, whereas others do not, and may even apply solo components of the resistance management program. We investigated whether growers using solo components of resistant management programs affect the durability of disease control in fields of those who implement fungicide resistance management. We developed a spatially implicit semidiscrete epidemiological model for the development of fungicide resistance. The model simulates the development of epidemics of spot-form net blotch disease, caused by the pathogen *Pyrenophora teres* f. *maculata*. The landscape comprises three types of fields, grouped according to their treatment program, with spore dispersal between fields early in the cropping season. In one field type, a fungicide resistance management method is implemented, whereas in the two others, it is not, with one of these field

types using a component of the fungicide resistance management program. The output of the model suggests that the use of component fungicides does affect the durability of disease control for growers using resistance management programs. The magnitude of the effect depends on the characteristics of the pathosystem, the degree of inoculum mixing between fields, and the resistance management program being used. Additionally, although increasing the amount of the solo component in the landscape generally decreases the lifespan within which the resistance management program provides effective control, situations exist where the lifespan may be minimized at intermediate levels of the solo component fungicide.

Keywords: alternations, ascospores, conidia, DMI, fungicide effective life, fungicide treatment programs, gene flow, *Hordeum vulgare*, mixtures, net blotch, *Pyrenophora teres* f. *maculata*, SDHI, solo, spatially implicit semidiscrete epidemiological model

Alternations and mixtures (whether as a result of substituting a fungicide and keeping the total fungicide dose of an application program constant or adding a fungicide and increasing the total dose; van den Bosch et al. 2014) of fungicides with different modes of action (MOAs) are widely recognized as effective resistance management methods. Consider, for example, a treatment program consisting of two applications per season of a solo fungicide A. Replacing one of these applications with a fungicide with another MOA—resulting in an alternation—reduces the time the pathogen is exposed to fungicide A and thereby reduces selection for resistance to the MOA of fungicide A. Alternatively, adding a mixing partner with another MOA to the solo fungicide reduces the rate of growth of the epidemic, thereby reducing the rate of increase in the frequency of the resistance to fungicide A

(van den Bosch et al. 2014). An extensive review of the experimental and theoretical evidence that alternation and mixtures are effective resistance management methods is published in van den Bosch et al. (2014). However, all the evidence accumulated so far relates to cases where the pathogen population receives the same treatment program in every field. No spores from a pathogen population that has been under a different fungicide application program enter the pathogen population under consideration. In other words, the pathogen population under consideration is a closed population. In practice, fungal spores can travel hundreds of meters up to 10 s of kilometer distances through the air (Agrios 2005). For example, ascospores of the pathogen *Zymoseptoria tritici*, causing Septoria blotch on wheat, and *Pyrenophora teres* f. *maculata*, causing spot-form net blotch on barley, produced at the start of the crop-growing season travel easily between fields.

Within the limits set by a regulator, growers can decide which fungicide application program they use, independent of other growers. This results in a mosaic of treatment programs throughout the landscape. Many growers will follow general resistance management advice and use mixtures or alternations. However, there will always be some growers that do not use such resistance management methods. There may be a range of reasons a grower would choose to apply only a single fungicide to their fields, including the larger costs of mixtures, lack of knowledge of resistance management advice, and timing constraints. Spores produced by a pathogen population in fields not following resistance management recommendations are likely to reach nearby fields where growers use alternations or mixtures as resistant management strategies. Whether growers using single components of resistant management programs affects the durability of disease control in the fields of growers using alternations or mixtures is something that still needs to be explored.

†Corresponding author: J. Helps; joe.helps@rothamsted.ac.uk

Funding: Support for F. van den Bosch, A. Zerihun, and F. Lopez-Ruiz was provided by the Centre for Crop and Disease Management, a joint initiative of Curtin University of Technology and the Grains Research and Development Corporation (research grant CUR00023). Support for J. Helps was provided by two UKRI grants: Smart Crop Protection Strategic Program 401 (BBS/OS/CP/000001) and the Growing Health Institute Strategic Programme (BB/X010953/1 and BBS/E/RH/230003C) funded by the Biotechnology and Biological Sciences Research Council. Rothamsted Research receives strategic funding from the Biotechnology and Biological Sciences Research Council of the United Kingdom.

e-Xtra: Supplementary material is available online.

The author(s) declare no conflict of interest.

In this study, we explored the scenario described above, using spot-form net blotch, caused by the pathogen *P. teres* f. *maculata*, on barley systems in Western Australia as a case study. This pathogen has emerged as a major disease of barley worldwide, probably as a consequence of reduced or no-tillage practices and increased susceptibility of cultivars (Mathre et al. 1997; McLean et al. 2009; Shipton et al. 1973). Spot-form net blotch can cause typical yield losses of 10 to 40% (Mathre et al. 1997; Murray and Brennan 2010). Epidemics are initiated at the start of each growing season by initial inoculum, which consists of both sexually produced ascospores from stubble infected at the end of the previous season, and asexual conidia from stubble and other volunteer host plants. Subsequent secondary cycles during the crop-growing season are driven by conidia. *P. teres* f. *maculata* lesions initially develop through biotroph-like growth but then switch quickly to necrotrophic growth (Backes et al. 2021), and the production of spores takes place in dead leaf tissue (Shipton et al. 1973).

For many important diseases, fungicide applications remain the main method of disease control. A wide range of fungicide MOAs are applied to control spot-form net blotch, including quinone-outside inhibitor fungicides (QoIs), dicarboximides, demethylation inhibitors (DMIs, a group containing most azoles), and succinate dehydrogenase inhibitors (SDHIs). In less productive areas, with lower annual rainfall, growers typically apply one foliar application of fungicide in a growing season. In higher yielding areas, with higher annual rainfall, growers normally use two foliar applications. These foliar applications are often tank or preformulated mixtures, but growers sometimes decide to use a solo fungicide on the basis of cost or other considerations. For example, an application of propiconazole costs on average \$6/ha. The price of the spray per hectare might easily be doubled when growers try to protect the azole from eroding in efficacy by tank mixing with azoxystrobin, for example. The introduction of the SDHI fluxapyroxad as a seed treatment improved the control of spot-form net blotch significantly (McLean and Hollaway 2019). The application of an SDHI seed treatment together with propiconazole foliar applications is a commonly used alternation of SDHI and azole fungicides. The combination of SDHIs and propiconazole is widely utilized among barley growers, as it is the most cost-effective approach to the chemical management of net blotch and other pathogens. The seed dressing SDHI has demonstrated a long-lasting disease control effect that allows growers to delay the application of a foliar fungicide.

The use of fungicides exerts selection pressures on the pathogen population, leading to the evolution of pathogen strains with reduced sensitivity to them. As with many pathogens, this has happened with net blotch. Resistance to the fungicide propiconazole developed in spot-form net blotch in the field in two ways. An insertion in the promoter region of the gene coding for Cyp51 developed that has a reduced sensitivity to propiconazole. Strains have also developed that have mutations in the coding region of the gene. These strains also have a reduced sensitivity to propiconazole (Mair et al. 2016, 2020). Subsequently, strains have been found with both the insertion and the mutation that have a high level of resistance to propiconazole (Mair et al. 2016, 2020). The strains with low levels of resistance are still sensitive to azoles to such an extent that no loss of efficacy was observed in the field. A study by van den Bosch et al. (2023) also showed that these resistant strains do not affect the yield and cost due to the disease in any significant way. We therefore only consider the highly resistant strains in our model. These highly resistant strains do affect field performance and even result in the azole fungicide propiconazole no longer being economically justified once this strain has come to dominate the population (van den Bosch et al. 2023). For the SDHI resistance, the situation is very similar, with an intermediate resistant strain developing and a highly resistant strain that does cause a high level of field failure (observations by the authors). For the SDHI, we also only consider the highly resistant strain.

In this paper, we present a spatially implicit semidiscrete epidemiological model of spot-form net blotch, in which epidemics of spot-form net blotch develop within fields in a landscape, with fields implementing one of three treatment programs and spore dispersal between fields. One set of fields implements a resistance management program, either an alternation or mixture, whereas another set uses a solo component of that resistance management program (the third set uses a treatment program with an alternative MOA and is present to ensure a constant total field size within the landscape). By varying the proportion of fields in the landscape using a component of the resistance management strategy and measuring the effective life of the disease control in the fields using mixtures/alternations, we quantify the effect of component use on the durability of disease control in those fields using mixtures/alternations as a resistance management method.

Although spot-form net blotch controlled by the fungicides propiconazole and fluxapyroxad is our study example, we examine parameter values beyond this particular case to see how generalizable the results are. Specifically, we use two sets of dose response curves, one fit to the available data and one partially representing the data, to create two cases: Case 1, where the treatment program loses effective control (to be defined below) when resistance to both fungicides has developed to high frequencies, and Case 2, where effective control can be lost when resistance develops to only one of the fungicides. We also consider the cases where there is more sexual reproduction than typically seen in spot-form net blotch and examine the effect of different amounts of inter-field spore mixing on the results.

Materials and Methods

Overview of the model

Crop, pathogen, and fungicide dynamics. The model keeps track of the host and the pathogen over a series of years/crop-growing seasons, in three groups of fields. The years are numbered by n , and the time within a year is denoted by t . Where possible, we suppress the index n for clarity. The model consists of two phases, within the growing season and between growing seasons. Within each growing season, the model describes the development of the barley canopy, with growth and senescence in thermal time. Initial inoculum increases in density at the start of each growing season and infects the growing crop canopy. Following infection with the initial inoculum, several secondary pathogen cycles develop. The main effect of the pathogen is a reduction in the green leaf area duration of the crop and therewith the amount of assimilate available to build up grain, thereby reducing yield. Control of the pathogen is carried out with fungicides, and the fungicides we consider are systemic fungicides, which affect the transmission rate of the pathogen (the product of the sporulation rate and infection efficiency) and the length of the latent period. Fungicide resistance is incorporated into the model for two of these fungicides. Between seasons, the pathogen survives over winter as inoculum on stubble from previous crops and on volunteer plants in the area. The model was written as a package in R, and the code is available on GitHub (Helps 2023). A graphical representation of the model is given in Figure 1. State variables are summarized in Table 1.

The spatial layout

There are three groups of fields, each receiving a different fungicide treatment program, with a seed treatment and two foliar applications. The field groups will be denoted by index K . We will suppress the index K where possible to avoid notational clutter. We consider three fungicides: (i) an SDHI fungicide (parameterized as fluxapyroxad), (ii) an azole fungicide (parameterized as propiconazole), and (iii) another fungicide of further unspecified nature.

We assume that field group 1 covers half the total area in the landscape and receives a fungicide resistance management program.

This program is either (i) an alternation treatment where an SDHI (fluxapyroxad) is used as seed treatment, an azole (propiconazole) as the first foliar treatment, and a treatment with the third fungicide to complete the program, or (ii) a mixture treatment with each fungicide at half dose compared with when used solo, where mixtures of SDHI and azole are used in the first foliar application and the seed treatment, and second foliar applications use the third fungicide. In field group 2, one of the fungicides to which resistance develops, SDHI or azole, is used as a solo product in one application—when the SDHI is used as the resistance management component, it is applied as a seed treatment; when the azole is the resistance management component, it is applied as the first foliar application—and the other two applications use the third fungicide. Field group 3 receives three applications of the third fungicide. Field group 3 is present for the following reason: If we only include the first two field groups, an increase in the number of growers using solo products would automatically decrease the number of growers using alternations or mixtures. In that case, when evaluating the dynamics in fields of group 1, we could not adjust the proportion of fields in the landscape using resistance management and using component or alternative products independently. By introducing the third group of fields, we keep the number of growers in fields of group 1 constant. Our previous modeling work has been criticized for only including the MOA of interest in simulations designed to simulate the development of resistance to that MOA, leading to unrealistic under-controlled pathogen epidemics where a different fungicide would have been used. Moreover, in practice, a considerable fraction of barley growers use a QoI and dicarboximide-based fungicide program, which is represented by fields in group 3 using the third fungicide. To account for this, we introduce a third fungicide to

our model, which we apply at times where a fungicide application would normally take place but the fungicides under consideration are not used. This third fungicide is thus only present to align the treatment programs with practice. We do not consider the development of resistance to this fungicide. The dose response curves of this third fungicide are chosen to reflect folpet—a multisite to which no resistance is known—which has recently been registered for use in barley but is any fungicide used in the landscape that is neither of the two under consideration in terms of resistance management. The treatment programs are summarized in Table 2. We have chosen the treatment programs to reflect the practically applied treatment programs on barley against net blotch in Western Australia.

To investigate the effect of growers only using a solo product and the third fungicide in their treatment program on the durability of disease control for growers who use an alternation or a mixture, we increase the area of field group 2 gradually from a fraction $Z = 0$ to $Z = 0.5$ (Fig. 2) and observe how this affects the durability of control in field group 1.

Pathogen genotypes

We consider one mutation to a high level of resistance for each of the fungicides propiconazole and fluxapyroxad. We thus have to consider four pathogen strains: a strain susceptible to both fungicides, SS; a strain sensitive to propiconazole and resistant to fluxapyroxad, SR; a strain resistant to propiconazole and sensitive to fluxapyroxad, RS; and a strain resistant to both, RR. We will use SS, SR, RS, and RR as subscripts i, j in the model equations to indicate the strain under consideration. Mutations can take place in the genotypes. When a mutation occurs in one nucleus in a cell of a pathogen lesion, this will have little effect on the genotype

Fig. 1. Graphical representation of the model. H is the healthy canopy area, L is the canopy area with latent infections, I is the canopy area with infectious infections, and R is the amount of canopy removed due to the disease or senescence. The dynamics are shown with no fungicides applied. The inset graph shows the shape of the initial inoculum curve over time.

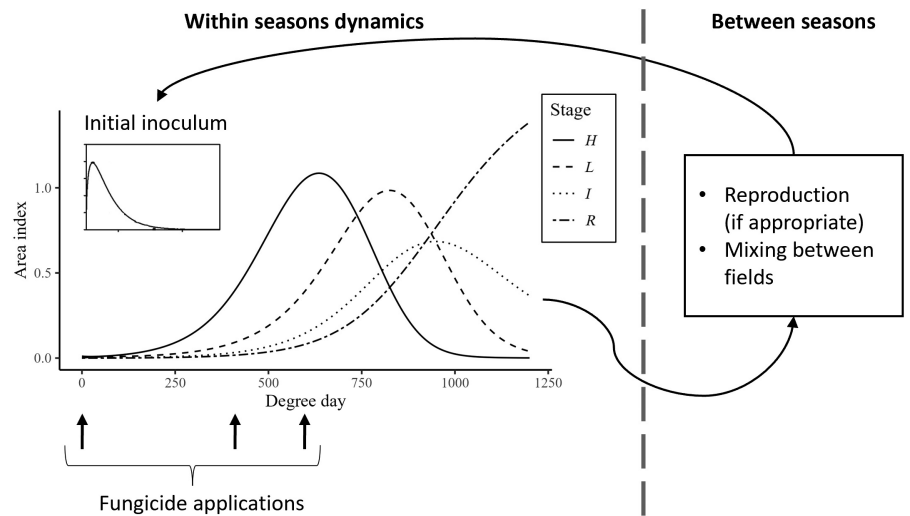


TABLE 1. The four scenarios studied in the paper^a

Scenario	Field group	Seed treatment	First foliar	Second foliar
1. Alternation in field group 1, azole in field 2	1	Succinate dehydrogenase inhibitor (SDHI)	Azole	Third fungicide
	2	Third fungicide	Azole	Third fungicide
	3	Third fungicide	Third fungicide	Third fungicide
2. Alternation in field group 1, SDHI in field 2	1	SDHI	Azole	Third fungicide
	2	SDHI	Third fungicide	Third fungicide
	3	Third fungicide	Third fungicide	Third fungicide
3. Mixture in field group 1, azole in field 2	1	Third fungicide	SDHI + azole	Third fungicide
	2	Third fungicide	Azole	Third fungicide
	3	Third fungicide	Third fungicide	Third fungicide
4. Mixture in field group 1, SDHI in field 2	1	Third fungicide	SDHI + azole	Third fungicide
	2	Third fungicide	SDHI	Third fungicide
	3	Third fungicide	Third fungicide	Third fungicide

^a Each scenario has a specific fungicide treatment program in each of the field groups.

composition of the population, as in the vast majority of cases, this mutant cell will not lead to the production of offspring because most cells in a lesion do not produce spores. The way mutations lead to offspring with a different genotype is when mutations take place in spores/sporophores/etc. We therefore include a mutation rate in the spore production and transmission terms.

Measuring durability

We measure the durability of a disease control program, in our case a fungicide treatment program, using the effective life (van den Bosch et al. 2014). The effective life is defined as the time span between the introduction of the fungicide treatment program and the moment effective disease control is lost due to the build-up of resistance. We consider effective disease control to be lost when disease-induced yield loss passes a preset threshold. It has been established (Bingham et al. 2019) that for barley crops, the healthy area duration (HAD, the healthy area integrated over time) of the entire canopy (from sowing to harvest) is well correlated with yield. This healthy area duration is a measure of the potential total amount of carbon assimilation by the canopy during the entire cropping season. We thus define effective disease control to be lost when more than 10% of the healthy area duration is lost to disease.

Within growing season dynamics

Canopy dynamics. Following Milroy and Goyne (1995), we describe crop canopy growth over time with a logistic curve, and, later on in the season, the senesced leaf area also increases logistically. With the growth rate and the senescence rate denoted by $g(t)$ and

$s(t)$, respectively, equation 1 describes the dynamics of the green leaf area (H):

$$\frac{dH}{dt} = g(t) - s(t) \quad (1)$$

where we suppressed the field group index K , noting that canopy dynamics in all field groups are the same. In equation 1,

$$g(t) = \frac{H_{\max} r e^{-r(t-m_g)}}{(1 + e^{-r(t-m_g)})^2}$$

and

$$s(t) = \frac{H_{\max} r e^{-r(t-m_s)}}{(1 + e^{-r(t-m_s)})^2}$$

with H_{\max} being the maximum green canopy index, r the canopy growth rate per unit canopy area, m_g the time of onset of canopy growth, and m_s the time of onset of canopy senescence. Unlike in Milroy and Goyne (1995), we have a shared rate of increase parameter, r , for both the growth rate and the senescence rate, as the fit was sufficient with just one shared parameter. Note that $g(t)$ and $s(t)$ are the total canopy rates of growth and senescence, not per capita rates. The senescence term appears in the equation describing the dynamics of the uninfected canopy area and the latently infected canopy area but not in the equation of the infectious area, as sporulation takes place on dead leaf tissue, and thus, senescence does not affect this area.

The initial inoculum. The rate of deposition of initial inoculum onto the crop per unit area, $\psi(t)$, is described by a gamma-density-like function in equation 2:

$$\psi(t) = \Psi \frac{t^{\eta-1} e^{-\frac{t}{\lambda}}}{\Gamma(\eta)\lambda^\eta} \quad (2)$$

where we have again suppressed the field group index K . Ψ is the total (time integrated) density of ascospores produced by one unit of crop area, η is the shape parameter, and λ is the time scaling parameter.

The genotype composition of the initial inoculum varies each year, n . Denoting the fractions of each of the genotypes in the initial inoculum in field group K in year n by $\theta_{ij}^{(K)}$, where ij is SS, SR, RS, or RR as described above, the rate of deposition of each genotype at time t is described in equation 3, being the product of the rate of deposition of all the initial inoculum at time t and the genotype frequency of the initial inoculum in field group K in year n :

$$\psi_{ij}^{(K)}(t) = \theta_{ij}^{(K)} \psi^{(K)}(t) \quad (3)$$

The frequency of the genotypes in the initial inoculum is made up of spores resulting from asexual conidial clonal reproduction and those from sexual reproduction from ascospores. The initial inoculum is generated between growing seasons, when no crop is growing in the fields. The dynamics between crop-growing seasons are explained in a section below.

Dynamics of healthy, latent, and infectious area. The canopy area is divided into healthy (uninfected), $H(t)$; latently infected, $L(t)$; infectious/sporulating, $I(t)$; and senesced, $R(t)$. We describe

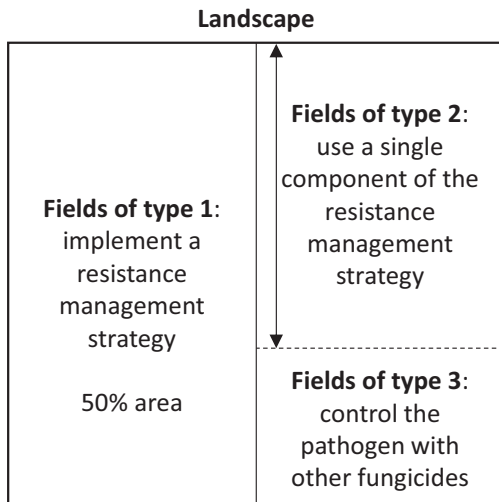


Fig. 2. The structure of the landscape. There are three groups of fields. Fields of type 1 receive the treatment with the two fungicides to which resistance is developing. Fields of type 2 receive a treatment with one of the two fungicides to which resistance is developing. Fields of type 3 receive treatments with the third fungicide only. The black arrow indicates increasing or decreasing the area of fields of type 2; this is the variable studied in the manuscript and plotted on the x axis of Figures 5 and 6. Full treatment programs are in Table 2.

TABLE 2. State variables in the model

Symbol	Variable
H	Healthy area index
L_{ij}	Area index of the canopy that is latently infected by net blotch pathogen, specifically a strain that has alleles i and j
I_{ij}	Area index of the canopy that is latently infected by net blotch pathogen, specifically a strain that has alleles i and j
R	Area index of the canopy that has senesced or that is no longer infectious
$D_{l \in \{a,s,3\}}$	The dose of fungicide l in the leaf canopy, where l may be the azole (a), the succinate dehydrogenase inhibitor (s), or the third fungicide (3)
$\theta_{cl}^{(K)}_{ij n-1}$	The genotype frequency of asexual clonal conidial spores in field K in year $n-1$, the genotype consisting of alleles i and j
$\theta_{se}^{(K)}_{ij n-1}$	The genotype frequency of sexual ascospores in field K in year $n-1$, the genotype consisting of alleles i and j

the dynamics of these canopy areas without including mutations. In the next paragraph, we explain how mutations are included.

As described in equation 1, the healthy canopy area increases due to canopy growth and decreases due to canopy senescence. The healthy area also decreases following infections from the initial inoculum or secondary infections from the subsequent epidemic. The rate of deposition of the initial inoculum is described by Ψ_{ij} , and each unit of infectious leaf tissue, I_{ij} , produces α spores per time unit, where the indexes i and j refer to the alleles of each resistance gene. The sum $\alpha I_{ij} + \Psi_{ij}$ thus denotes the total number of (asco- and conidio-) spores of type ij deposited on the canopy per time unit. Summing up over ij gives the total rate of deposition of pathogen spores. A spore landing on the canopy has a probability equal to the fraction of the canopy that is healthy, $F_H(t)$,

$$F_H(t) = \frac{H}{H + \sum_{ij} L_{ij} + \sum_{ij} I_{ij}}$$

to land on an uninfected piece of tissue. We assume here, as no other information is available, that the probability of infection once a spore has landed on a healthy piece of leaf tissue, the infection efficacy β_{ij} , is the same for ascospores and conidiospores. Note, as mentioned previously, that the infection efficiency depends on the doses of the two fungicides, $D_a(t)$ and $D_s(t)$, in the canopy at the moment of infection. The equation modeling the dynamics of the healthy area is therefore given in equation 4:

$$\begin{aligned} \frac{dH}{dt} = & g(t) - s(t)F_H(t) \\ & - \sum_{i,j} (\beta_{ij}(D_a(t), D_s(t))(\alpha I_{ij} + \Psi_{ij}))F_H(t) \end{aligned} \quad (4)$$

The function $s(t)$ is the total senescence rate and therefore needs to be multiplied by the fraction of the canopy that is healthy to remove the correct amount of healthy leaf area. Note that an assumption here is that the growth rate of healthy canopy is not affected by the disease. Disease mainly has the effect of reducing the photosynthetically active canopy area. An experiment by Beed et al. (2007) showed, using shading screens in the field, that canopy dynamics are unaffected when the amount of incoming radiation is reduced by up to 50%. This underpins our assumption.

The density of latent infected leaf area, which is divided between the four genotypes, increases due to the infections on the healthy leaf area and decreases due to lesions reaching the end of the latent period and due to leaf area senescing. The mean length of the latent period is given by $1/\mu$. The equation modeling the dynamics of the latently infected leaf area is therefore given by equation 5:

$$\begin{aligned} \frac{dL_{ij}}{dt} = & \beta_{ij}(D_a(t), D_s(t))(\alpha I_{ij} + \Psi_{ij})F_H(t) - \\ & \mu_{ij}(D_a(t), D_s(t))L_{ij} - s(t)F_L(t) \end{aligned} \quad (5)$$

where $F_L(t)$ is the fraction of the leaf area that is latently infected,

$$\frac{\sum_{ij} L_{ij}}{H + \sum_{ij} L_{ij} + \sum_{ij} I_{ij}}$$

Note that the latent period is dependent on the dose of the two fungicides present in the canopy, $\mu_{ij}(D_a(t), D_s(t))$.

The density of infectious leaf area in the canopy increases when latent lesions become infectious sporulating lesions and decreases when infectious lesions reach the end of their infectious period. The mean infectious period is $1/\omega$. Equation 6 describes the dynamics of the infectious leaf area:

$$\frac{dI_{ij}}{dt} = \mu_{ij}(D_a(t), D_s(t))L_{ij} - \omega I_{ij} \quad (6)$$

Mutations. Mutations from the sensitive to the resistant allele take place at a rate ε . We assume the mutation rates to be equal and independent for the azole and the SDHI resistance, as no information on this quantity exists. The mutation rate of SS to RR is equal

to ε^2 . Therefore, altering the transmission rate according to Table 3, the rate of change of the latent area index of SS strains is described by equation 7:

$$\begin{aligned} \frac{dL_{SS}}{dt} = & \left(\begin{array}{l} (1 - 2\varepsilon - \varepsilon^2)\beta_{SS}(D_a(t), D_s(t))(\alpha I_{SS} + \Psi_{SS}) + \\ \varepsilon\beta_{SR}(D_a(t), D_s(t))(\alpha I_{SR} + \Psi_{SR}) + \\ \varepsilon\beta_{RS}(D_a(t), D_s(t))(\alpha I_{RS} + \Psi_{RS}) + \\ \varepsilon^2\beta_{RR}(D_a(t), D_s(t))(\alpha I_{RR} + \Psi_{RR}) \end{array} \right) F_H(t) \\ & - \mu_{SS}(D_a(t), D_s(t)) - s(t)F_L(t) \end{aligned} \quad (7)$$

and is similar for the other genotypes. The mutation expression is also incorporated into equation 4.

The effect of fungicides. We use the equations describing the effect on the pathogen's life-cycle parameters as we have previously (Hobbelen et al. 2011a, b; van den Berg et al. 2013). In short, the fungicides decrease the infection efficiency, β , and increase the length of the latent period, $1/\mu$. We assume no effect of the fungicide on the infectious period. Using the usual exponential dependence of the parameter value on fungicide dose, gives equations 8a and b:

$$\beta(D(t)) = \beta_0(1 - RD + RDe^{-kD(t)}) \quad (8a)$$

$$\mu(D(t)) = \mu_0(1 - RD + RDe^{-kD(t)}) \quad (8b)$$

where β_0 and μ_0 are the infection efficiency and the rate of transition from latent to infectious when no fungicides are applied, $1 - RD$ is the asymptotic efficacy of the fungicide (at infinite dose), and k is the shape parameter. We assume that the action of the SDHI and the azole are independent and of a multiplicative nature (Paveley et al. 2003). Making equations 8a and b genotype specific and including the two fungicides, gives equations 9a and b:

$$\beta_{ij}(D_a(t), D_s(t)) = \quad (9a)$$

$$\beta_0(1 - RD_{ai} + RD_{ai}e^{-k_{ai}D_a(t)})(1 - RD_{sj} + RD_{sj}e^{-k_{sj}D_s(t)})$$

$$\mu_{ij}(D_a(t), D_s(t)) = \quad (9b)$$

$$\mu_0(1 - RD_{ai} + RD_{ai}e^{-k_{ai}D_a(t)})(1 - RD_{sj} + RD_{sj}e^{-k_{sj}D_s(t)})$$

where index a mean azole and index s means SDHI. Because fungicide 3 is always applied alone, the effect of fungicide 3 is described by equations 10a and b:

$$\beta_{ij}(D_3(t)) = \beta_0(1 - RD_3 + RD_3e^{-k_3D_3(t)}) \quad (10a)$$

$$\mu_{ij}(D_3(t)) = \mu_0(1 - RD_3 + RD_3e^{-k_3D_3(t)}) \quad (10b)$$

Fungicides can be applied at three points in time. First, a seed treatment can be used. Then, two foliar sprays are applied, the first at T1, which is crop growth stage 31, GS31, which corresponds to thermal time 400, and the second at T2, which is GS39, which corresponds to thermal time 600. Following a foliar fungicide application, the dose in the canopy is instantaneously increased by the value of the application dose, D_i . Due to UV light, rain, and plant metabolism, this dose gradually decreases to zero as described by equation 11:

$$\frac{dD_i}{dt} = -\xi_i D_i \quad (11)$$

where i is a , s , or 3 and ξ_i is the decay parameter for fungicide i .

TABLE 3. Table with mutation frequencies of the genotypes

Strain	SS	SR	RS	RR
SS	$1-2\varepsilon-\varepsilon^2$	ε	ε	ε^2
SR	ε	$1-2\varepsilon-\varepsilon^2$	ε^2	ε
RS	ε	ε^2	$1-2\varepsilon-\varepsilon^2$	ε
RR	ε^2	ε	ε	$1-2\varepsilon-\varepsilon^2$

When applied as seed treatments, the dynamics of the fungicide dose are a little more complicated. The fungicide around the seed is slowly taken up by the root and distributed through the plant. Kitchen et al. (2016) modeled these fungicide dynamics in two different mechanistic ways and showed that the qualitative conclusions were insensitive to the precise description. We therefore take recourse to a simple description and assume that the dose in the plant tissue is described by

$$\frac{dD_i}{dt} = D_0 \frac{t^{m-1} e^{-\frac{t}{\delta}}}{\Gamma(m)\delta^m} - \xi_i D_i \quad (12)$$

where the dose increases due to uptake of the fungicide from the seed and then gradually decreases until all fungicide is depleted. Moreover, the fungicide decays in the same way as the foliar applied fungicide with rate ξ_i (equation 12).

Between growing season dynamics. Between growing seasons, the pathogen survives on crop stubble and volunteers. The pathogen population on these sources consists of infections from the previous growing season, as well as some pathogens that survived from the growing season before that. Pathogens from each growing season reproduce either clonally or sexually or a combination of these two, and the inoculum consists of the combination of spores from both years. The inoculum spores leave the field and mix with spores from fields from the other field groups. This spore mixture then forms the initial inoculum.

We describe the genotype frequency of the initial inoculum that initiates the epidemic in year n and how it relates to the genotype frequency at the end of years $n - 1$ and $n - 2$.

Asexual and sexual reproduction. In the following, variables relating to asexual conidial clonal reproduction are labeled cl , and those relating to sexual reproduction from ascospores are labeled se . For those spores in the initial inoculum that were produced clonally from conidia, the genotype frequency in the inoculum produced on the stubble during the crop-free season in a field of type K , $\theta_{cl\ ij\ n-1}^{(K)}$ is the same as the genotype frequency at the end of the previous growing season in that field group (equation 13).

$$\theta_{cl\ ij\ n-1}^{(K)} = \theta_{ij\ n-1\ \text{end of season}}^{(K)} \quad (13)$$

For those spores produced from sexual reproduction, we use the gene recombination frequencies for haploid organisms (Crow and Kimura 1970; Wijngaarden et al. 2005), and so, the frequency of a genotype in the inoculum produced on the stubble between growing seasons in a field of type K , $\theta_{se\ ij\ n-1}^{(K)}$, is given by equations 14a and b, where ii indicates a homozygous genotype and ij indicates a heterozygous genotype:

$$\theta_{se\ ii\ n-1}^{(K)} = \theta_{ii\ n-1\ \text{end of season}}^{(K)} - \phi D \quad (14a)$$

$$\theta_{se\ ij\ n-1}^{(K)} = \theta_{ij\ n-1\ \text{end of season}}^{(K)} + \phi D, \quad i \neq j \quad (14b)$$

where

$$D = \theta_{SSn-1\ \text{end of season}}^{(K)} \theta_{RRn-1\ \text{end of season}}^{(K)} - \theta_{SRn-1\ \text{end of season}}^{(K)} \theta_{RSn-1\ \text{end of season}}^{(K)} \quad (15)$$

The parameter ϕ is the recombination rate, which for independent genes is 0.5. Combining the clonal and sexually produced spores, we denote that a fraction, c , of the inoculum produced on the stubble in a field of type K is clonal, and a fraction, $1 - c$, is sexually produced (equation 16).

$$\theta_{ij\ n-1}^{(K)} = c\theta_{cl\ ij\ n-1}^{(K)} + (1 - c)\theta_{se\ ij\ n-1}^{(K)} \quad (16)$$

Between field spore mixing. To incorporate long-distance dispersal of the inoculum produced between growing seasons, we need to calculate the genotype composition of the cloud of spores above the fields. Assume a fraction B of the inoculum does not travel far

and remains in the field in which it was produced, and a fraction $(1 - B)$ becomes airborne for a longer period of time and may leave the field. The genotype frequency of the airborne spores is given by equation 17:

$$\theta_{ij\ n-1} = \left(\frac{1}{2} \theta_{ij\ n-1}^{(1)} + Z\theta_{ij\ n-1}^{(2)} + \left(\frac{1}{2} - Z \right) \theta_{ij\ n-1}^{(3)} \right) \quad (17)$$

We assume, therefore, that each field contributes spores to the spore cloud according to its area and the severity in that field at the end of the previous growing season—specifically the severity on the last day of the growing season—because the severity determines how much stubble is infected and therefore how many spores are going into the cloud. We define severity as the proportion of the senescence-free crop that is infections, $\frac{I}{H+L+I}$. The relative contribution of the spores from fields K is then thus (area-of- $K \times$ severity-in- K)/ Σ (area-of- $K \times$ severity-in- K), as described by equations 18, 19, and 20:

$$\theta_{ij\ n-1} = \left(A1\theta_{ij\ n-1}^{(1)} + A2\theta_{ij\ n-1}^{(2)} + A3\theta_{ij\ n-1}^{(3)} \right) \quad (18)$$

where

$$A1 = \frac{\left(\frac{1}{2} \frac{\sum_{ij} I_{ij}^{(1)}}{H + \sum_{ij} L_{ij}^{(1)} + \sum_{ij} I_{ij}^{(1)}} \right)}{T} \quad (19a)$$

$$A2 = \frac{\left(Z \frac{\sum_{ij} I_{ij}^{(2)}}{H + \sum_{ij} L_{ij}^{(2)} + \sum_{ij} I_{ij}^{(2)}} \right)}{T} \quad (19b)$$

$$A3 = \frac{\left(\left(\frac{1}{2} - Z \right) \frac{\sum_{ij} I_{ij}^{(3)}}{H + \sum_{ij} L_{ij}^{(3)} + \sum_{ij} I_{ij}^{(3)}} \right)}{T} \quad (19c)$$

where T is the total amount of infectious leaf area in the landscape:

$$T = \frac{1}{2} \frac{\sum_{ij} I_{ij}^{(1)}}{H + \sum_{ij} L_{ij}^{(1)} + \sum_{ij} I_{ij}^{(1)}} + Z \frac{\sum_{ij} I_{ij}^{(2)}}{H + \sum_{ij} L_{ij}^{(2)} + \sum_{ij} I_{ij}^{(2)}} + \left(\frac{1}{2} - Z \right) \frac{\sum_{ij} I_{ij}^{(3)}}{H + \sum_{ij} L_{ij}^{(3)} + \sum_{ij} I_{ij}^{(3)}} \quad (20)$$

The genotype frequencies in the initial inoculum in field group K in year n from year $n - 1$ (equation 21) are therefore given by the combination of equations 16 and 18.

$$\theta_{ij\ n}^{(K)} = B\theta_{ij\ n-1}^{(K)} + (1 - B)\theta_{ij\ n-1} \quad (21)$$

Stubble survival. However, due to the dry conditions in many years in Western Australia, stubble/debris can sometimes survive for more than a year on the soil. Therefore, a fraction P of the initial inoculum develops on debris from 2 years ago and the remaining fraction $1 - P$ of the initial inoculum is from last year, and incorporating this into equation 21 gives equation 22.

$$\theta_{ij\ n}^{(K)} = P \left(B\theta_{ij\ n-2}^{(K)} + (1 - B)\theta_{ij\ n-2} \right) + (1 - P) \left(B\theta_{ij\ n-1}^{(K)} + (1 - B)\theta_{ij\ n-1} \right) \quad (22)$$

Parameterization

Throughout the parameterizations, time is measured in degree days. This is because many processes in the crop and the pathogen scale with temperature.

The canopy dynamics were fitted to data in Kamali and Boyd (2000). Measurements of canopy area index were scaled from the 2 years of data so that the maximum canopy density was scaled to 1 to fit the growth and senescence rates and midpoints, and the maximum canopy density parameter in the model (H_{\max}) was set to the average of the maximum of the 2 years. Time was measured

in degree days since coleoptile emergence on 1 October. Parameters were estimated, here and elsewhere, by minimizing the sum of squared errors between the observed and predicted values, using the optim function in R. Figure 3A shows the fits of the model to the data, and the parameter values are provided in Table 4.

There is surprisingly little information on the latent period (with-out fungicide use) and the infectious period of this pathogen. Shaw (1986) estimated latent periods of net blotch but did not distinguish between spot- and net-form. With a mean temperature of 20°C during the growing season, Shaw (1986) reported a latent period of 9 days, whereas McLean et al. (2009) estimated 14 days, giving an average of 12 days and a thermal time of 225 degree days. No estimates of the infectious period are available. Two experts (Mike Shaw, Reading University, U.K., and Geoff Thomas, Department of Primary Industries and Rural Development, Western Australia) suggested using the same length as the latent period, 225 degree days.

No data were found about initial inoculum density/deposition over time. The initial inoculum timing parameter λ was set so that 99.9% of the initial inoculum was produced during the first half of the season. We set $\eta = 1$, resulting in an exponential decay of the initial inoculum over time. The remaining parameters for the infection process β_0 , α , and ψ were estimated by fitting the model to the epidemic dynamics data from Martin et al. (1993), which provided severity over four replicates. Figure 3B shows the resulting fit.

Fantke et al. (2014) reported a half-lifetime of propiconazole of 5.4 days, giving for the fungicide decay rate in degree day terms $\xi_a = 0.00856$. For fluxapyroxad, He et al. (2016) and Noh et al. (2019) gave half-lives of an average of 9 days. For this fungicide, we use $\xi_s = 0.0051$.

The dose response curves measuring the effect of fungicide dose on the infection efficiency and the latent period are parameterized on the basis of foliar application experiments. As far as we know, there are no experimental data available on the dose response of

SDHI as a seed treatment. The dose response curves of sensitive and resistant strains are different, and for propiconazole, we use the data set from van den Bosch et al. (2023). These dose response curves were measured in Western Australia in 2020. The fit of the dose response curve to the available data is given in Figure 3C.

For fluxapyroxad, dose response curve data from Western Australia are not available. We therefore used data from the fungicide performance trials in the United Kingdom (<https://ahdb.org.uk/fungicide-performance-guide>), which relate to foliar applications. The appropriate dose data of 2012, 2013, and 2014 were averaged to give the dose response curve for the sensitive strain. No data exist on the dose response curve of the pathogen strains resistant to fluxapyroxad. We only have EC_{50} (the concentration fungicide at which the growth of the pathogen is reduced by 50%) lab data on the resistant strain. Rehfus (2018) measured an EC_{50} of the wild type, WT, of 0.005 and an EC_{50} of the highly resistant, HR, strain of 0.3 to 0.5, so the resistant strain has a resistance factor of 60 to 100. Similarly, data in Mair et al. (2016, 2020) give an EC_{50} for the WT of 0.0087 and for an HR strain of 1.234, giving a resistance factor of 143. We therefore used a resistance factor of 100 as an average value. This resistance factor is used to calculate the relative severity versus dose response curve for the resistant strain from those of the sensitive strain. The model was fitted to all four dose response curves to estimate the parameters, see Table 4 and Figure 3C, D, and E. These dose response curves are used for Case 1, where resistance to both fungicides needs to develop before effective disease control is lost. For Case 2, where the development of resistance to only one of the two fungicides is required before effective control is lost, we made a mock-up parameter set, in which the asymptotes of the sensitive strain dose-response curves were changed to the SDHI and the third fungicide. The gray lines in Figure 3 show the dose response curve for this mock-up data set.

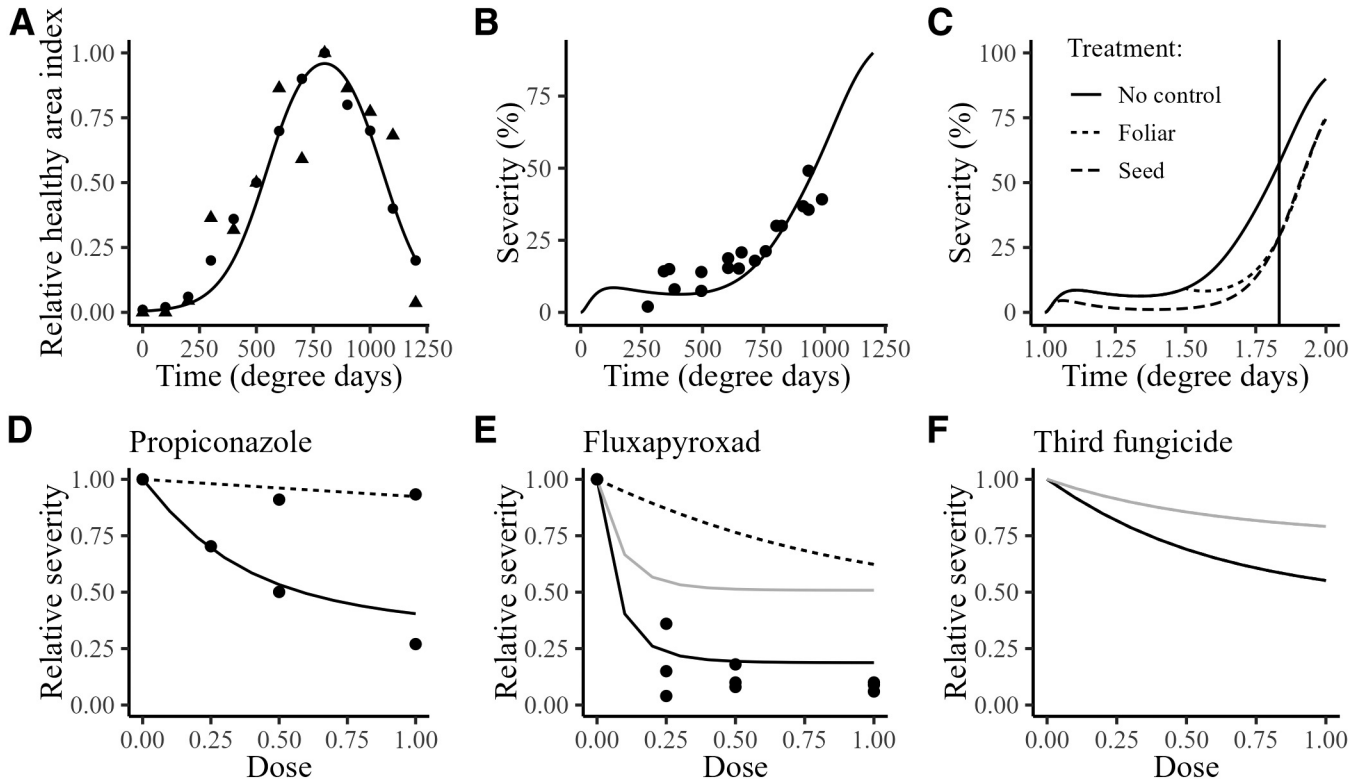


Fig. 3. Graphs with the data and the fit of the model to the data. **A**, Canopy dynamics in the absence of disease ($R^2 = 0.874$; root mean square error [RMSE] = 0.120). **B**, Fit of the model to the epidemic data ($R^2 = 0.680$; RMSE = 6.88). **C**, Simulations showing the effect of both a seed treatment and a T1 foliar spray, showing that the effect of a seed treatment is equal to that of a T1 spray. **D**, Dose response curves for propiconazole. The solid line is the sensitive strain ($R^2 = 0.939$; RMSE = 0.068), and the hashed line is the resistant strain ($R^2 = 0.690$; RMSE = 0.038). **E**, Dose response curves for fluxapyroxad ($R^2 = 0.934$; RMSE = 0.098). The solid black line is the sensitive strain, and the hashed black line is the resistant strain. The gray line is the hypothetical dose response curve used for Case 2 (described in main text). **F**, The dose response curves of the third fungicide.

Finally, to parameterize the effectiveness of a seed treatment, the only information we found is that a seed treatment with fluxapyroxad is about as effective as a spray at GS31 (McLean and Hollaway 2019; Platz et al. 2017; Simpfendorfer 2017). We adjusted the parameters of the seed treatment so that the severity at 1,000 degree days for a model simulation with a seed treatment applied matched the model output of a foliar spray at GS31 (Fig. 3C).

Results

Figure 3 shows the fit of the model to the various data sets. Figure 3A and B shows that the model describes the canopy dynamics of an uninfected crop and the epidemic dynamics in an infected crop accurately. The graphs in the bottom row of Figure 3 show the fit of the model to the dose response data. Note that we do not have data for the resistant strain of fluxapyroxad, as resistance to fluxapyroxad

TABLE 4. Parameter values used in the model^a

Parameter	Interpretation	Value	Reference(s)
Landscape			
Z	Fraction of the landscape of field group 2, the fields treated with a solo fungicide	0–0.5	–
B	Fraction of initial inoculum leaving the field	0.25, 0.5, 1.0	–
Crop growth			
H_{\max}	Maximum green canopy index	2.75	Kamali and Boyd 2000
r	Canopy growth rate per unit canopy area	0.01	Kamali and Boyd 2000
m_g	Time of onset of canopy growth	550	Kamali and Boyd 2000
m_s	Time of onset of canopy senescence	1,050	Kamali and Boyd 2000
Pathogen life cycle			
β_0	Infection efficiency of spores	0.12	Model fit, see main text
α	Rate of spore production of an infectious lesion	0.4	Model fit, see main text
$1/\mu_0$	Mean latent period in the absence of fungicides	225	Shaw 1986; McLean et al. 2009
$1/\omega$	Mean infectious period	225	M. Shaw, <i>personal communication</i>
Mutation			
ε	Mutation rate	10^{-7}	Chosen arbitrarily
Initial, inoculum			
Ψ	Total initial inoculum density deposited	0.13	Model fit, see main text
λ	Time scale parameter of the initial inoculum	40	99.9% of initial inoculum deposited before 1 July
η	Shape parameters of the initial inoculum	1	Assuming exponential decay of initial inoculum
P	Fraction of infected stubble surviving 2 years after production	0.1	Bhathal and Loughman 2001
Sexual recombination			
ϕ	Recombination fraction	0.5	–
c	The fraction of overwinter inoculum that reproduces clonally	0.0	–
Fungicide decay rates			
ξ_a	Decay rate of propiconazole	0.006	Model fit, see main text
ξ_s	Decay rate of fluxapyroxad	0.00513	Model fit, see main text
ξ_3	Decay rate of third fungicide	0.006	Model fit, see main text
Fungicide dose response curves, Case 1			
Propiconazole			
RD_{aS}	Asymptote, sensitive strain	0.69	Model fit, see main text
k_{aS}	Curvature parameter, sensitive strain	6.27	Model fit, see main text
RD_{aR}	Asymptote, resistant strain	0.86	Model fit, see main text
k_{aR}	Curvature parameter, resistant strain	0.26	Model fit, see main text
Fluxapyroxad			
RD_{sS}	Asymptote, sensitive strain	0.86	Model fit, see main text
k_{sS}	Curvature parameter, sensitive strain	27.9	Model fit, see main text
RD_{sR}	Asymptote, resistant strain	0.6	Model fit, see main text
k_{sR}	Curvature parameter, resistant strain	2.4	Model fit, see main text
The third fungicide			
RD_3	Asymptote, sensitive strain	0.6	Model fit, see main text
k_3	Curvature parameter, sensitive strain	4.00	Model fit, see main text
Fungicide dose response curves, Case 2 (changes only)			
Fluxapyroxad			
RD_{sS}	Asymptote, sensitive strain	0.5	Model fit, see main text
The third fungicide			
RD_{3S}	Asymptote, sensitive strain	0.3	Model fit, see main text
Seed treatment			
D_0	Total dose around the seed	Succinate dehydrogenase inhibitor: 0.8; third fungicide, 0.96	Model fit, see main text
m	Shape parameter	4	There is a slow onset of seed derived fungicide in the plant
δ	Timing parameter	20	Time to peak concentration is 200 degree days

^a Parameters, their interpretation, and their numerical value are given.

developed very recently. With this parameterization of the model, the build-up of resistance to either fluxapyroxad or propiconazole will end the effective life of the treatment program. The gray lines in Figure 3 are a different parameterization of the model, which corresponds to the case in which both fungicides need to develop resistance before effective disease control is lost.

Figure 4 shows the effect of a range of fungicide application programs on the canopy and disease dynamics. Figure 4A shows the situation where no fungicides are applied, and a severe epidemic develops ($HAD = 407$). Using a propiconazole T2 spray, Figure 4B shows that the disease is reduced, and the healthy canopy increases drastically ($HAD = 563$). When propiconazole is applied at T1 and T2, the healthy area increases further, and the disease is very strongly suppressed compared with a T1 spray only program ($HAD = 1,049$). Adding to these two foliar spray programs a seed treatment with fluxapyroxad reduces the disease to very low levels ($HAD = 1,192$) that have virtually no effect on yield anymore (without any pathogen, $HAD = 1,319$).

Figure 5 shows results for Case 1, where the build-up of resistance to both fungicides (fluxapyroxad, propiconazole) leads to the loss of effective disease control. Figure 6 shows results for Case 2, where the build-up of resistance to only one of the fungicides is needed before effective disease control is lost.

We first summarize the effects of parameters on the shape of the effective life curves that do not depend on the proportion of fields of type 2 in the system. Both Figures 5 and 6 show the following:

- i. The effective life of treatment programs where fungicides are used in mixtures are larger than those of alternations.
- ii. The smaller the proportion of spores in the initial inoculum in fields of type 1 coming from fields of types 2 and 3, the smaller the effective life of the fungicide treatment program.
- iii. There is little difference in the shape of the curves in Figures 5 and 6 when comparing the situation where azoles are used in fields of type 2 or SDHIs are used in fields of type 2.

In Figure 5, we see that depending on the other parameters (frequency of sexual reproduction, fraction of spores dispersing between fields), growers in fields of type 2 (where they only use one of the two fungicides under consideration) can have a considerable impact on the effective life of the treatment program applied by growers in fields of type 1, whether both fungicides are used in alternation or a mixture.

However, whether the effect of growers in fields of type 2 on the effective life of disease control for growers of type 1 is large or small strongly depends on other aspects of the pathosystem. For alternations, the effective life decreases as the proportion of fields of

type 2 increases in the landscape, although in the absolute number of years of effective life, the decrease is very small. For mixtures, the effective life either decreases with the proportion of fields of type 2 or first decreases and then increases again, in a u-shape.

By varying the proportion of the inoculum derived from sexual recombination and the amount of spore exchange between fields (parameters that are hard to parameterize from data), Figure 5 also shows the degree to which the results are generalizable.

- i. Increasing the proportion of the initial inoculum derived from sexual reproduction decreases the effective life more with increasing proportion of fields of type 2. In other words, the decrease in effective life with increasing proportion of fields of type 2 is larger for sexual reproduction than for clonal reproduction.
- ii. When the spore exchange between fields is smaller, spores from fields of type 2 have a smaller effect on the effective life of the treatment program in fields of type 1.

The trends in the effective life with the proportion of fields of type 2 in Case 2 (Fig. 6) are very similar to those in Case 1 (Fig. 5), with some exceptions:

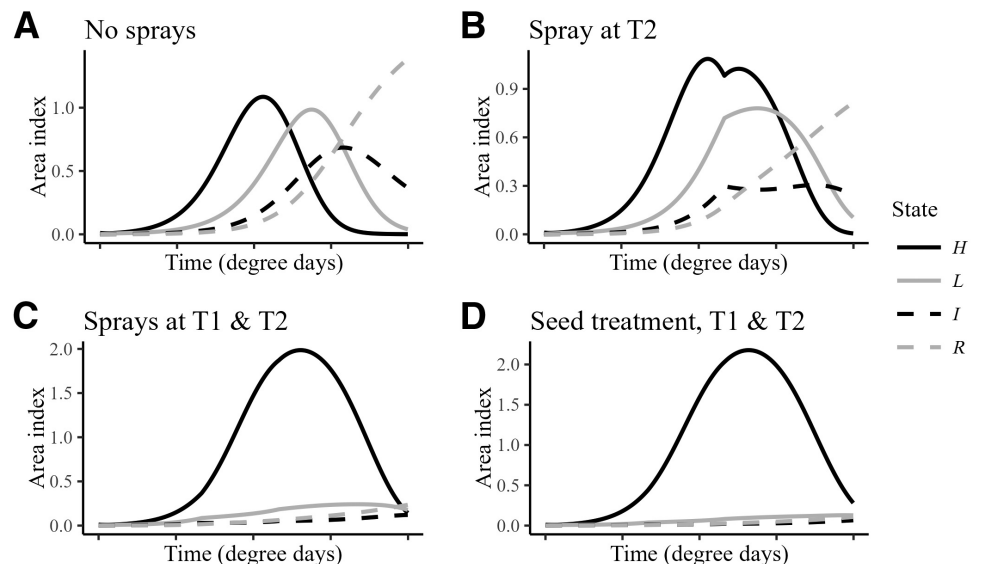
- i. There is very little effect of the proportion of fields of type 2 on the effective life in the case of alternating fungicides.
- ii. The effective life always decreases with increasing proportion of fields of type 2. The u-shape in some cases in Figure 5 is absent from Figure 6.

Figure 7 shows the dynamics of the four strains through time for a range of parameter values. This figure will help interpret the shape of the effective life versus proportion fields of type 2 curves. We address this further in the discussion section.

Discussion

A range of spatially implicit and spatially explicit epidemiological models to study plant disease control have been published (Fabre et al. 2015; Liu et al. 2017; Pacilly et al. 2018; Watkinson-Powell et al. 2020). For example, Fabre et al. (2015), Watkinson-Powell et al. (2020), and Pacilly et al. (2018) studied the effect of resistance gene deployment on the efficacy and durability of disease control. Gene deployment strategies such as pyramiding, mixing (growing cultivars with different resistance genes in fields), and mosaics (where each field contains one of a range of crop genotype) have been frequently compared in terms of their efficacy and durability (Rimbaud et al. 2021). Surprisingly, very few spatial epidemic models exist that study the effect of spatial differences on fungicide

Fig. 4. The effect of treatment programs on the development of the green/healthy canopy, the density of latent lesions, and the density of infectious lesions. **A**, No fungicide treatments applied; **B**, foliar propiconazole treatment applied at T2; **C**, foliar propiconazole spray applied at T1 and T2; **D**, seed treatment with fluxapyroxad and foliar treatments with propiconazole at T1 and T2. The solid black line is the healthy canopy area, the solid gray line is the area infected with pathogen in the latent stage, the dashed black line is the area in the infectious stage, and the dashed gray line is the crop area with removed pathogen. T1 is the timing of a fungicide application at growth stage 31 (GS31), which corresponds to 400 degree days, and T2 is the timing of a fungicide application at GS39, which corresponds to 600 degree days. *H*, healthy; *L*, latently infected; *I*, infectious/sporulating; and *R*, senesced.



treatment programs and the emergence and selection of fungicide resistance. This is despite evidence that much can be gained from including spatial considerations in the development of fungicide application programs (Liu et al. 2017). Furthermore, a long-term study, carried out in France from 2004 to 2017, on the evolution of fungicide resistance clearly showed that the major driver of resistance dynamics was fungicide use at the regional scale (Garnaut et al. 2021) and the spore exchange between fields and regions.

In this paper, we developed a spatially implicit semidiscrete epidemiological model with spore exchange between fields. We used this model by grouping those fields with the same fungicide treatment program, assuming that the spatial pattern of the fields is such that spore exchange between different types of fields is similar at all positions in the landscape. Those fields in group 1 receive a treatment with two fungicides to which resistance can develop, with these fungicides either alternated within a growing season or mixed. Fields of type 2 receive fungicide programs with only one of the fungicides to which resistance develops, and fields of type 3 have

programs that do not include the fungicides to which resistance develops.

The model shows that for all parameter combinations, the effective life when alternating the fungicides in fields of type 1 is smaller than when mixing the fungicides. Changing an alternation into a mixture requires splitting the dose of both fungicides and mixing them for application in each spray. It is well known that splitting fungicide dosages increases the selection for resistance and that mixing decreases the selection for resistance (van den Bosch et al. 2014). The balance between the increase and decrease of selection determines whether alternation or mixing will result in the longer effective life. In most cases that have been studied, the decrease in selection from mixing overshadows the increase in selection from splitting doses. van den Bosch et al. (2014) found six publications with a total of nine pathogen-crop-fungicide mixtures tested. In seven cases, the selection for fungicide resistance of the at-risk fungicide was reduced by the mixture. Our model shows an example where the additional protection against selection for resistance

Fig. 5. Effective life as a function of the proportion of fields of group 2. This graph is for the situation where the resistance to both fungicides needs to build up before effective disease control, Case 1, is lost. Top row, initial inoculum is derived from clonal reproduction; middle row, initial inoculum 50% clonal 50% sexual; bottom row, initial inoculum 100% sexual. Two left columns: alternation treatment in fields of type 1. Two right columns: mixture treatment in fields of type 1. First and third columns: propiconazole used in fields of type 2; second and fourth columns: fluxapyroxad used in fields of type 2. Solid line: fraction of the spore of the initial inoculum leaving the field and being deposited in other fields 20%; dotted line: 50%; and dashed line: 100%.

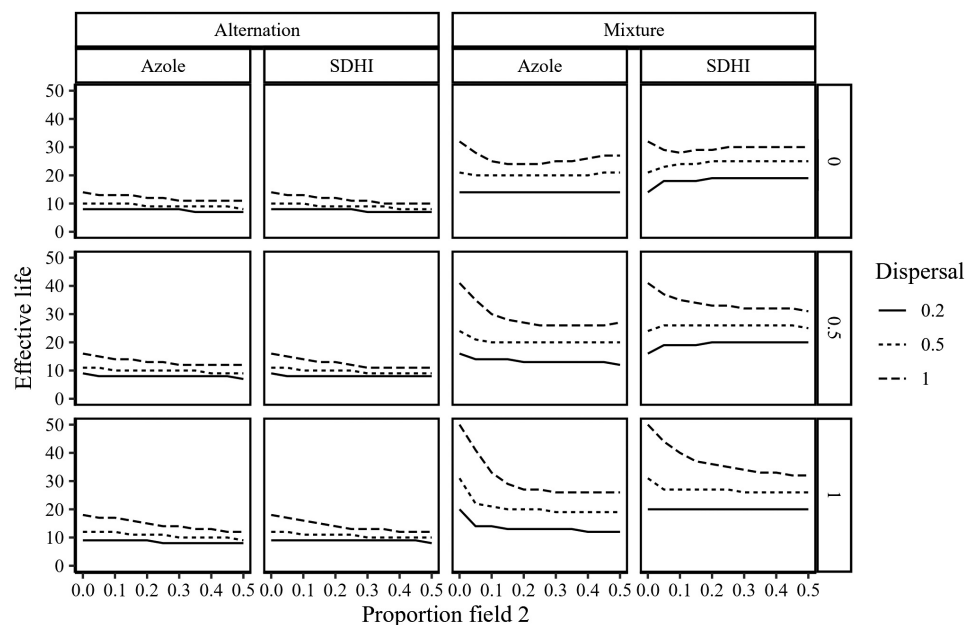
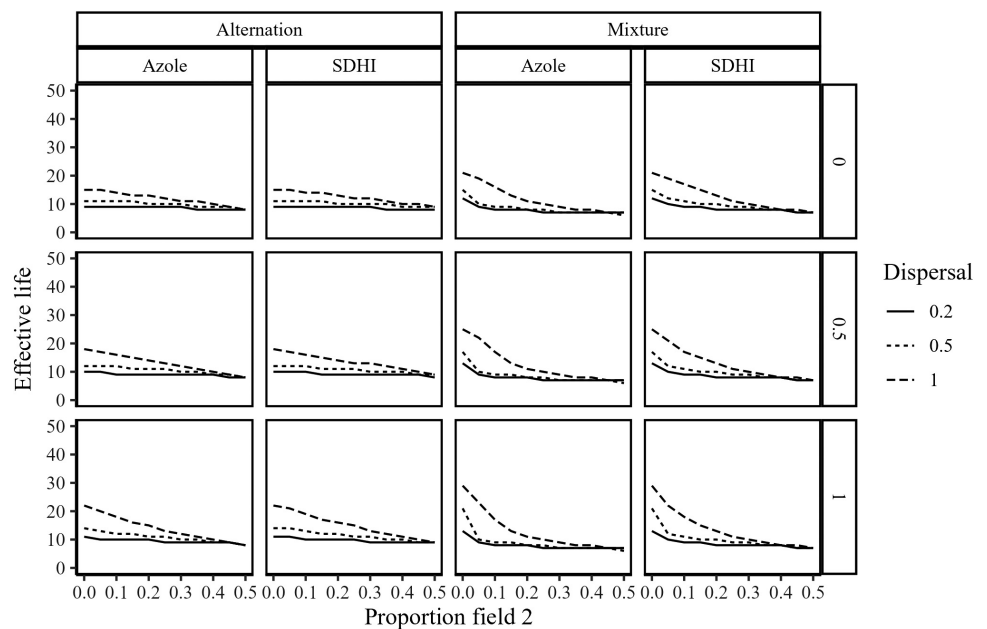


Fig. 6. Effective life as function of the proportion of fields of group 2. This graph is for the situation where the resistance to one of the fungicides can lead to the loss of effective disease control, Case 2. Top row, initial inoculum is derived from clonal reproduction; middle row, initial inoculum 50% clonal 50% sexual; bottom row, initial inoculum 100% sexual. Two left columns: alternation treatment in fields of type 1. Two right columns: mixture treatment in fields of type 1. First and third columns: propiconazole used in fields of type 2; second and fourth columns: fluxapyroxad used in fields of type 2. Drawn line: fraction of the spore of the initial inoculum leaving the field and being deposited in other fields 20%; dotted line: 50%; and dashed line: 100%.



due to mixing clearly outweighs the increase in selection due to splitting dosages.

Figures 5 and 6 also show that a smaller degree of spore exchange between the fields reduces the effective life of the fungicide treatment program in fields of type 1. Furthermore, the effective life becomes virtually independent of the proportion of fields of type 2 when spore exchange between fields is small. Both these observations can be explained by the same mechanism. When fewer spores arrive from other fields, the spores generated in fields of type 1 are less diluted. This implies that the selection that took place during the growing season is not diluted by spores immigrating from the other two field types. This results in a faster increase in the fraction of resistance in the pathogen population and therewith a shorter effective life of the fungicide treatment program. Additionally, a smaller spore immigration rate decouples fields of type 1 from the dynamics of fields of types 2 and 3. The effect of this is that the effective life becomes less sensitive to the fungicide programs in fields of type 2 when the spore exchange is small.

The patterns in Figures 5 and 6 for the cases where propiconazole is used in type 2 fields and the case where SDHIs are used are qualitatively similar. Remember that in the case of alternation, the SDHI is used as a seed treatment and the azole as a foliar spray. Our results are therefore shown to be independent of the fungicide used, as well as whether the fungicide is applied as a seed treatment or foliar spray. This makes it possible to apply our findings to a wider range of cases. Kitchen et al. (2016) and Brent et al. (1989) also found that the selection for resistance does not differ between fungicides applied as seed treatments or foliar sprays. Kitchen et al. (2016) developed a model of *Zymoseptoria tritici* epidemics in wheat, with both seed and foliar applications of fluquinconazole, and calculated that the increase in the frequency of resistance is the same whether the fungicide is applied as a seed treatment or as a single foliar spray. To date, Brent et al. (1989) reported the only plot-field experiment measuring selection for resistance of seed treatment and foliar sprays. They showed that the selection for resistance to triadimenol in powdery mildew of barley is the same for a seed treatment or one foliar spray. Given these results, it is not surprising that our results do not depend on whether propiconazole or fluxapyroxad was used in type 2 fields.

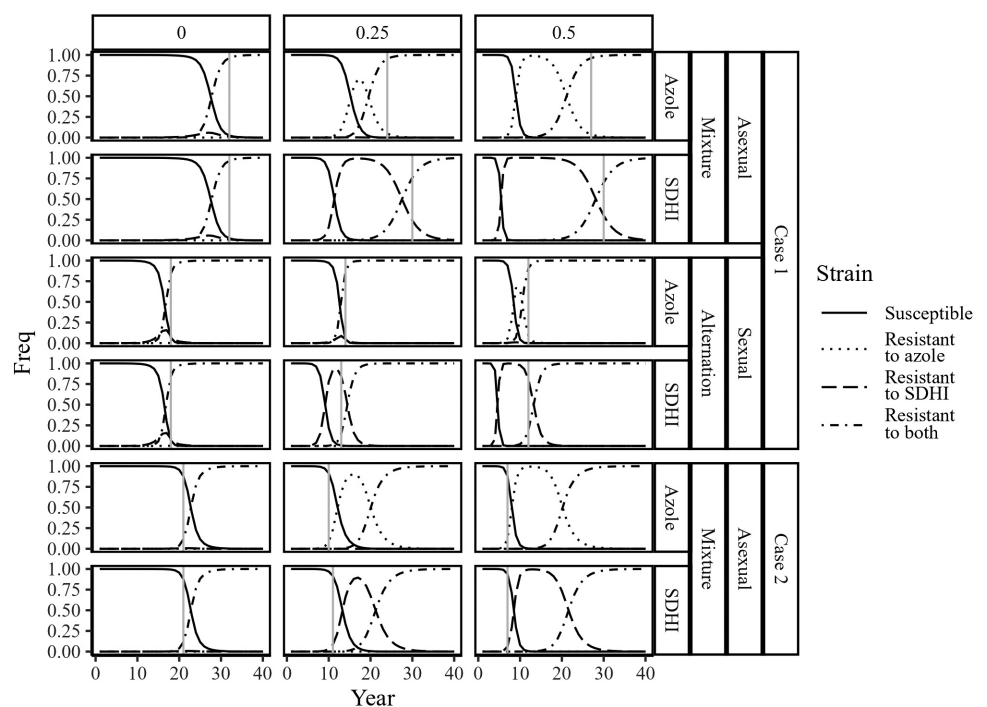
One factor that can potentially affect the effective life is the rate of mutation. To evaluate this, we set the mutation rate to a value typical for the range of the point mutation rate of a nucleotide. Other genetic changes can have an effect on fungicide resistance levels, such as insertions in the promoter region of the Cyp51-coding gene of net blotch. We therefore did model simulations with increased mutation rates. We did not find qualitative differences in the consequences of increasing the proportion of fields of type 2, although higher mutation rates result in an overall shorter effective life (see Supplementary Material for results).

Similarly, there is no information on possible fitness costs of net blotch strains resistant to azoles and/or SDHIs. To explore possible effects should fitness costs exist, we carried out some simulations with a larger-than-zero fitness cost (the transmission rate being reduced by 1 and 0.1%). These results are shown in the Supplementary Material. As for mutation rates, there were no qualitative differences in the results.

The objective of this work was to understand whether growers in fields of type 2—using only one of two possible fungicides to which resistance develops—affect the durability of disease control for growers in fields of type 1, who use the fungicides in either a rotation or a mixture. The results clearly show that growers not using mixtures or rotations can reduce the effective life of the treatment program of growers who use mixtures or alternations. The extent of this effect does, however, strongly depend on the treatment program.

In all cases, when the fraction of the initial inoculum produced through sexual reproduction is large, the effective life of the treatment program is larger than for smaller contributions of sexual reproduction to the initial inoculum, although in the case of alternation, the differences are very small. This phenomenon is well known in population genetics (Roughgarden 1995). The effective life is, in Case 1, terminated as a result of the strain resistant to both fungicides taking over the fungal population. When both the alleles conferring resistance are rare in the pathogen population, any strain carrying both resistance alleles will almost certainly mate with a strain sensitive to both fungicides, resulting in offspring strains resistant to only one of the fungicides. In this way, sexual reproduction delays the emergence of the strain resistant to both fungicides, which in turn increases the effective life of the treatment program.

Fig. 7. Dynamics of the four genotypes in the pathogen population over time (thermal time in degree days) in several scenarios. The four genotypes are susceptible (solid black, the pathogen genotype is sensitive to both fungicides), resistant to azole (dotted, the pathogen is resistant to propiconazole and sensitive to fluxapyroxad), resistant to the succinate dehydrogenase inhibitor (SDHI) (dashed, pathogen genotype is resistant to fluxapyroxad and sensitive to propiconazole), and both (dot and dash, pathogen genotype is resistant to both propiconazole and fluxapyroxad). Each column represents a different proportion of the landscape that contains field 2, the field using components of the resistance management program. Each row denotes a specific simulation: either mixture or alternation in fields of type 1 (Mix or Alt); SDHI or azole used in fields of type 2 (SDHI or azole); and either clonal or sexual reproduction. The vertical gray line indicates when control was lost.



In Figure 5, the curve of the effective life for a range of proportions of fields of type 2 is u-shaped when the between-season reproduction is clonal. When the fraction of sexual reproduction contributing to the initial inoculum increases, this u-shape disappears, and with only sexual reproduction contributing to the initial inoculum, it is a monotonically decreasing curve. The explanation for this is clarified in Figure 7. First, consider the u-shape when reproduction is clonal. When there are no fields of type 2 (Fig. 7, left column), the resistance to both fungicides starts at very low frequencies. Resistant strains are then selected from this population, in fields of type 1 alone. Because the pathogen population is confronted with only mixtures, the only strain that has a high phenotype of resistance is the strain resistant to both fungicides. It is this strain that, after some time, appears in the population and will eventually dominate the pathogen population, thereby ending the effective life of the treatment program. However, when 25% of the fields are of type 2 (Fig. 7, middle column), the strain resistant to the MOA used in fields of type 2 (for example, fluxapyroxad) is selected for in fields of type 2. Due to dispersal between the fields, a subpopulation of strains resistant to that MOA, fluxapyroxad, builds up in fields of type 1. The strain resistant to both fungicides has a large fitness advantage in the population, as the majority of pathogen strains are sensitive, with only a small proportion being resistant to fluxapyroxad. Because of the relatively high frequency of the strain resistant to fluxapyroxad, a mutation resulting in a strain resistant to both fungicides is more likely to occur. This causes the strain resistant to both fungicides to appear about 8 years earlier in the pathogen population in fields of type 1, resulting in a shorter effective life.

However, when 50% of the landscape is made up of fields of type 2 (Fig. 7, right column), the population of strains resistant to fluxapyroxad builds up quickly, as fluxapyroxad is now used alone in a large proportion of the landscape. This results in the fluxapyroxad-resistant strain taking over the pathogen population in fields of type 1 almost completely by year 7. Contrary to when 25% of the fields is of type 2, the double-resistant strain now has a much smaller fitness advantage because the population is already entirely resistant to fluxapyroxad. The selection pressure is therefore smaller for the double-resistant strain to emerge. The consequence is that it emerges after 23 years and builds up a subpopulation more slowly than it did in the case where 25% of the field are of type 2. This results in a longer effective life, hence the u-shape curve of the effective life versus the proportion of fields of type 2.

The pathogen population consists, for a long time, of only the strain resistant to fluxapyroxad. The frequencies of the other strains are very small. That this happens is surprising because the only stable steady state in the system is that of the pathogen population consisting of strains resistant to both fungicides. However, because the mutation rate is very small, the double-resistant strain takes a long time to emerge. This results in the population moving very close to the unstable steady state where the frequency of the fluxapyroxad resistant strain is close to 1. Even though unstable steady states are by definition unstable, and trajectories will move away from them, when close to a steady state, such changes are very slow, causing the population to remain for a long time close to unstable steady states. This phenomenon is well known from ecology, although not much studied (Cushing et al. 1998).

When the pathogen's initial inoculum consists entirely of inoculum from sexual reproduction, the situation is different (Fig. 5, bottom row, mixture). Here, the effective life decreases monotonically with an increasing proportion of fields of type 2, and the u-shape disappears. The key difference with the clonal case is that the strain resistant to both fungicides emerges much faster in the sexual than in the clonal case. Sexual reproduction prevents the system from moving close to the unstable steady state where the frequency of the strain resistant to only one of the fungicides becomes very close to 1 (Fig. 7), with recombination meaning the doubly resistant strains emerge much faster. We therefore have a dichotomy, where,

as discussed above, sexual recombination in general increases the effective life of the control program, as doubly resistant strains mating with susceptible strains slows the selection for the doubly resistant strains; however, by preventing the development of populations dominated by a single strain, sexual reproduction can, under specific circumstances, decrease the effective life of a control program.

The u-shape also does not appear in Case 2, where resistance must develop only to one fungicide before effective control is lost. The effective life ends when the frequency of the strain resistant to one of the fungicides has increased sufficiently (Fig. 6). Figure 7 shows that with clonal reproduction, the dynamics of the various strains are very similar to the strain dynamics, as the effective life only ends when resistance to both fungicides reaches high levels (Fig. 7). Why, then, is the u-shape not present? The reason is that the effective life ends when the strain resistant to only one of the fungicides has reached higher frequencies. It is not necessary for the double-resistant strain to emerge and grow to higher frequencies as in Case 1.

The effect of growers' choices of fungicide treatment program on the effectiveness of other growers' treatment programs has not been studied, so it is not possible to compare our results with any previous fungicide resistance literature. However, studies are available considering cultivar resistance, where the resistance gene protects the plant against pathogen infection and the pathogen evolves virulence to the resistant cultivar. Lof et al. (2017) and Lof and van der Werf (2017) considered the situation where many growers use cultivars with two pyramided resistance genes, whereas another group of growers use cultivars with the same resistance genes deployed singly. Lof et al. (2017) showed that even a small fraction of growers using the cultivar with only one resistance gene affects the durability of resistance of the pyramid to a great extent. This finding is consistent with our findings. Indeed, for the case of cultivar resistance, an experimental study is also available. Zhao et al. (2005) studied transgenic broccoli plants carrying two pyramided *Bacillus thuringiensis* genes effective against diamondback moth (*Plutella xylostella*). Plant populations with the pyramided plants alone were compared with populations with both the pyramid and some plants carrying only one of the two genes. The diamondback moth population overcame the cultivar resistance more slowly in the plant population with only pyramided genes compared with the plant population with both plants with the pyramided genes and plants with only a single resistance gene.

Our results thus lead to the conclusion that growers using solo fungicides in their fields can affect the durability of disease control for those growers using alternations and mixtures. This effect is much smaller for growers using alternations than for growers using mixtures. The currently most frequently used fungicide program for the control of net blotch on barley in Western Australia is an alternation where an SDHI fungicide is used as a seed treatment and an azole fungicide is used as a foliar application. Whether the effect of growers using solo fungicides on growers using mixtures is small or large depends on the characteristics of the pathosystem. Key parameters are sexual versus clonal reproduction generating the initial inoculum and the degree of initial inoculum dispersal between fields. Given the size of barely fields in Western Australia, the amount of spore exchange between fields becomes an important topic. It is currently not known how much spore exchange there is between fields in this system, and research in this area is needed.

Recently, mixtures of SDHI and azole fungicides have been registered for foliar use on barley in Australia. It is these mixtures whose effective life will be most compromised by the use of solo fungicides by some of the growers.

Acknowledgments

We thank the anonymous reviewers for their efforts and revisions, which have improved the manuscript considerably.

Literature Cited

- Agrios, G. N. 2005. Plant Pathology. 5th ed. Elsevier, Amsterdam, the Netherlands.
- Backes, A., Guerriero, G., Ait Barka, E., and Jacquard, C. 2021. *Pyrenophora teres*: Taxonomy, morphology, interaction with barley, and mode of control. *Front. Plant Sci.* 12:614951.
- Beed, F. D., Paveley, N. D., and Sylvester-Bradley, R. 2007. Predictability of wheat growth and yield in light-limited conditions. *J. Agric. Sci.* 145:63-79.
- Bhathal, J. S., and Loughman, R. 2001. Ability of retained stubble to carry-over leaf diseases of wheat in rotation crops. *Aust. J. Exp. Agric.* 41:649-653.
- Bingham, I. J., Young, C., Bounds, P., and Paveley, N. D. 2019. In sink-limited spring barley crops, light interception by green canopy does not need protection against foliar diseases for the entire duration of grain filling. *Field Crop Res.* 239:124-134.
- Brent, K. J., Carter, G. A., Hollomon, D. W., Hunter, T., Locke, T., and Proven, M. 1989. Factors affecting build-up of fungicide resistance in powdery mildew in spring barley. *Neth. J. Plant Pathol.* 95:31-41.
- Crow, J. F., and Kimura, M. 1970. An Introduction to Population Genetic Theory. Harper & Row, New York.
- Cushing, J. M., Dennis, B., Desharnais, R. A., and Costantino, R. F. 1998. Moving toward an unstable equilibrium: Saddle nodes in population systems. *J. Anim. Ecol.* 67:298-306.
- Fabre, F., Rousseau, E., Mailleret, L., and Moury, B. 2015. Epidemiological and evolutionary management of plant resistance: Optimizing the deployment of cultivar mixtures in time and space in agricultural landscapes. *Evol. Appl.* 8:919-932.
- Fantke, P., Gillespie, B. W., Juraske, R., and Joliet, O. 2014. Estimating half-lives for pesticide dissipation from plants. *Environ. Sci. Technol.* 48:8588-8602.
- Garnault, M., Duplaix, C., Leroux, P., Couleaud, G., David, O., Walker, A.-S., and Carpentier, F. 2021. Large-scale study validates that regional fungicide applications are major determinants of resistance evolution in the wheat pathogen *Zymoseptoria tritici* in France. *New Phytol.* 229:3508-3521.
- He, M., Jia, C., Zhao, E., Chen, L., Yu, P., Jing, J., and Zheng, Y. 2016. Concentrations and dissipation of difenoconazole and fluxapyroxad residues in apples and soil, determined by ultrahigh-performance liquid chromatography electrospray ionization tandem mass spectrometry. *Environ. Sci. Pollut. Res. Int.* 23:5618-5626.
- Helps, J. 2023. Net Blotch Package, v0.0.1. Zenodo 8184541.
- Hobbelen, P., Paveley, N., Fraaije, B. A., Lucas, J. A., and van den Bosch, F. 2011a. Derivation and testing of a model to predict selection for fungicide resistance. *Plant Pathol.* 60:304-313.
- Hobbelen, P., Paveley, N., and van den Bosch, F. 2011b. Delaying selection for fungicide insensitivity by mixing fungicides at a low and high risk of resistance development: A modeling analysis. *Phytopathology* 101:1224-1233.
- Kamali, M. R. J., and Boyd, W. J. R. 2000. Quantifying the growth and development of commercial barley cultivars over two contrasting growing seasons in Western Australia. *Aust. J. Agric. Res.* 51:487-501.
- Kitchen, J. L., van den Bosch, F., Paveley, N. D., Helps, J., and van den Berg, F. 2016. The evolution of fungicide resistance resulting from combinations of foliar-acting systemic seed treatments and foliar-applied fungicides: A modeling analysis. *PLoS One* 11:e0161887.
- Liu, Y., Langemeier, M. R., Small, I. M., Joseph, L., and Fry, W. E. 2017. Risk management strategies using precision agriculture technology to manage potato late blight. *Agron. J.* 109:562-575.
- Lof, M. E., de Vallavieille-Pope, C., and van der Werf, W. 2017. Achieving durable resistance against plant diseases: Scenario analyses with a national-scale spatially explicit model for a wind-dispersed plant pathogen. *Phytopathology* 107:580-589.
- Lof, M. E., and van der Werf, W. 2017. Modelling the effect of gene deployment strategies on durability of plant resistance under selection. *Crop Prot.* 97:10-17.
- Mair, W. J., Deng, W., Mullins, J. G. L., West, S., Wang, P., Besharat, N., Ellwood, S. R., Oliver, R. P., and Lopez-Ruiz, F. J. 2016. Demethylase inhibitor fungicide resistance in *Pyrenophora teres* f. sp. *teres* associated with target site modification and inducible overexpression of *Cyp51*. *Front. Microbiol.* 7:1279.
- Mair, W. J., Thomas, G. J., Dodhia, K., Hills, A. L., Jayasena, K. W., Ellwood, S. R., Oliver, R. P., and Lopez-Ruiz, F. J. 2020. Parallel evolution of multiple mechanisms for demethylase inhibitor fungicide resistance in the barley pathogen *Pyrenophora teres* f. sp. *maculata*. *Fungal Genet. Biol.* 145:103475.
- Martin, R. J., Gillespie, R. N., and Knight, T. L. 1993. Prediction of reproductive growth stages in barley. *N. Z. J. Crop Hortic. Sci.* 21:73-84.
- Mathre, D. E., Kushnak, G. D., Martin, J. M., Grey, W. E., and Johnston, R. H. 1997. Effect of residue management on barley production in the presence of net blotch disease. *J. Prod. Agric.* 10:323-326.
- McLean, M. S., and Hollaway, G. J. 2019. Control of net form of net blotch in barley from seed- and foliar-applied fungicides. *Crop Pasture Sci.* 70:55-60.
- McLean, M. S., Howlett, B. J., and Hollaway, G. J. 2009. Epidemiology and control of spot form of net blotch (*Pyrenophora teres* f. *maculata*) of barley: A review. *Crop Pasture Sci.* 60:303-315.
- Milroy, S. P., and Goynes, P. J. 1995. Leaf area development in barley—Model construction and response to soil moisture status. *Aust. J. Agric. Res.* 46:845-860.
- Murray, G. M., and Brennan, J. P. 2010. Estimating disease losses to the Australian barley industry. *Australas. Plant Pathol.* 39:85-96.
- Noh, H. H., Lee, J. Y., Park, H. K., Lee, J. W., Jo, S. H., Lim, J. B., Shin, H. G., Kwon, H., and Kyung, K. S. 2019. Dissipation, persistence, and risk assessment of fluxapyroxad and penthiopyrad residues in perilla leaf (*Perilla frutescens* var. *japonica* Hara). *PLoS One* 14:e0212209.
- Pacilly, F. C. A., Hofstede, G. J., Lammerts van Bueren, E. T., Kessel, G. J. T., and Groot, J. C. J. 2018. Simulating crop-disease interactions in agricultural landscapes to analyse the effectiveness of host resistance in disease control: The case of potato late blight. *Ecol. Modell.* 378:1-12.
- Paveley, N. D., Thomas, J. M., Vaughan, T. B., Havis, N. D., and Jones, D. R. 2003. Predicting effective doses for the joint action of two fungicide applications. *Plant Pathol.* 52:638-647.
- Platz, G., Snyman, L., and Fowler, R. 2017. Seed treatments – Systiva® performance in northern trials. GRDC Grains Research Update 2017, Bellata. <https://grdc.com.au/resources-and-publications/grdc-update-papers/tab-content/past-update-proceedings/2017/grdc-grains-research-update-bellata-2017>
- Rehfus, A. 2018. Analysis of the emerging situation of resistance to succinate dehydrogenase inhibitors in *Pyrenophora teres* and *Zymoseptoria tritici* in Europe. Ph.D. thesis. Universität Hohenheim Institut für Phytomedizin.
- Rimbaud, L., Fabre, F., Papaix, J., Moury, B., Lannou, C., Barrett, L. G., and Thrall, P. H. 2021. Models of plant resistance deployment. *Annu. Rev. Phytopathol.* 59:125-152.
- Roughgarden, J. 1995. Theory of Population Genetics and Evolutionary Ecology: An Introduction. 1st ed. Benjamin Cummings, San Francisco.
- Shaw, M. W. 1986. Effects of temperature and leaf wetness on *Pyrenophora teres* growing on barley cv. Sonja. *Plant Pathol.* 35:294-309.
- Shipton, W. A., Khan, T. N., and Boyd, W. J. R. 1973. Net blotch of barley. *Rev. Plant Pathol.* 52:269-290.
- Simpfendorfer, S. 2017. Evaluation of fungicide management strategies to control spot-form of net blotch in barley. GRDC Grains Research Update 2017, Bellata. <https://grdc.com.au/resources-and-publications/grdc-update-papers/tab-content/past-update-proceedings/2017/grdc-grains-research-update-bellata-2017>
- van den Berg, F., van den Bosch, F., and Paveley, N. D. 2013. Optimal fungicide application timings for disease control are also an effective anti-resistance strategy: A case study for *Zymoseptoria tritici* (*Mycosphaerella graminicola*) on wheat. *Phytopathology* 103:1209-1219.
- van den Bosch, F., Oliver, R., van den Berg, F., and Paveley, N. 2014. Governing principles can guide fungicide-Resistance management tactics. *Annu. Rev. Phytopathol.* 52:175-195.
- van den Bosch, F., Zerihun, A., Poole, N., Thomas, G., and Lopez-Ruiz, F. J. 2023. Adjusting fungicide treatment programmes when resistance is developing: The case of spot-form net blotch in Western Australia. *Plant Pathol.* 72:1048-1058.
- Watkinson-Powell, B., Gilligan, C. A., and Cunniffe, N. J. 2020. When does spatial diversification usefully maximize the durability of crop disease resistance? *Phytopathology* 110:1808-1820.
- Wijngaarden, P. J., van den Bosch, F., Jeger, M. J., and Hoekstra, R. F. 2005. Adaptation to the cost of resistance: A model of compensation, recombination, and selection in a haploid organism. *Proc. Biol. Sci.* 272:85-89.
- Zhao, J.-Z., Cao, J., Collins, H. L., Bates, S. L., Roush, R. T., Earle, E. D., and Shelton, A. M. 2005. Concurrent use of transgenic plants expressing a single and two *Bacillus thuringiensis* genes speeds insect adaptation to pyramided plants. *Proc. Natl. Acad. Sci. U.S.A.* 102:8426-8430.